Mon. Not. R. astr. Soc. (1982) **199**, 345–354

Excising terrestrial radio interference in low frequency radio astronomy

B. L. Kasper,* F. S. Chute and D. Routledge *Department of Electrical Engineering, The University of Alberta, Edmonton, Canada T6G 2E1*

Received 1981 October 12; in original form 1981 August 4

Summary. Interference from terrestrial transmitters is a major problem in low-frequency radio astronomy. Experimental work is described in which a 22.25-MHz interferometer provided baseband signals from which 128-channel spectra were calculated in hardware by FFT and processed by a microcomputer. Narrow-band interference was identified and excised from the in-phase and quadrature cross-spectra and the auto-spectra in a 52-kHz band in real time. The observations were performed during winter near sun-spot maximum with the on-line microcomputer performing $\pm 4\sigma$ iterative deletion of interference. Off-line, an algorithm was developed in which robust estimation was used to give protection from statistical outliers.

The results showed consistently that 2–3 hr extra observing time were made possible per night. Low-level interference, which would not have been noticeable in records taken with a conventional receiving system, was detected and excised on most nights.

1 Introduction

The three major problems encountered by radio astronomers wishing to perform high-resolution, high-sensitivity observations at low frequencies are very large aperture dimensions, phase perturbations caused by the ionosphere, and interference from terrestrial transmitters. The first problem imposes no fundamental limitation, but does lead to practical difficulties. The Earth's ionosphere makes the other two problems difficult to escape for ground-based observers. Ionospheric effects could be eliminated by situating the telescope above the ionosphere, but terrestrial radio interference would remain unless the telescope could be installed in a shielded location such as the far side of the Moon.

Interference to ground-based observations is aggravated by the fact that, under typical conditions, terrestrial signals continue to reach the telescope by oblique reflection until the observing frequency is raised to about 3.6 times the ionospheric critical frequency. Historically, therefore, decametric ground-based observations have been largely restricted by

* Present address: Bell Telephone Laboratories, Holmdel, New Jersey, 07733, USA.

terrestrial interference to relatively 'quiet' bands a few tens of kHz wide; unfortunately, these become more difficult to find as the observing frequency is reduced (CCIR Report, 1976), because of increasingly heavy radio traffic.

Occasional attempts have been made in the past to build low-frequency telescopes capable of operating in the presence of narrow-band interference. Shain (1958) used four adjustable 4.5-kHz bandwidth filters with a 19.7-MHz Mills cross to select quiet gaps in a 100-kHz interval. An operator monitored the filter outputs with a loudspeaker and tuned the filters as required. In Tasmania (Ellis & Hamilton 1966; Hamilton & Haynes 1968) a 2–3 kHz wide bandpass filter sweeping five times per second through a 10–12 kHz spectral interval was used at 4.7 and 10.02 MHz with a minimum-detecting circuit to mitigate the effects of interference. Astronomical observations were made between transmitting stations, but with relatively poor sensitivity both to cosmic sources and to interfering signals because of conflicting constraints on the filter bandwidth used. Finally, the UTR-1 telescope at Grakovo (Braude *et al.* 1969) incorporated a variable bandwidth between 3 and 14 kHz, allowing the bandwidth to be reduced when interfering signals were noticed. Besides this, 'fast radiometer retuning' was employed when it became necessary to shift the reception band to avoid interference.

Auditory interference detection as used by Shain and by Braude *et al.* is undoubtedly very sensitive, but impracticable for earth-rotation synthesis observations requiring many hours' continuous data. On-line computer-based techniques are required which will allow much wider bandwidths to be used than those mentioned above, even in the presence of many interfering signals which contaminate a significant fraction of the reception band.

A previous experiment (Wheeler 1977) used off-line digital spectral analysis to reject narrow-band interference from recorded radio signals. The objective was to characterize the electromagnetic environment of the North Atlantic from 1.5 to 6.0 MHz, with a view to deleting interference from spread-spectrum radio transmissions. This problem is the same in principle as that faced in radio astronomy. Interplanetary-scintillation measurements (Duffett-Smith 1980) have also been made in the presence of narrow-band interference with a special 'correlating scintillometer' receiver.

In the following sections, we present details of an experiment in which a 128-channel cross-power FFT spectrometer was employed to excise narrow-band interference in real time from a 52-kHz spectral interval at 22.25 MHz (Kasper 1981). We report the results of interferometric observations of Cas A during the winter of 1979–80 which showed consistently that 2–3 hr additional observing time per night could be obtained near solar maximum. A robust-estimation procedure (Ershov 1979) employing maximum likelihood estimation (Huber 1964) was developed to remove interference from the in-phase and quadrature cross-spectra.

2 Equipment

2.1 THE ANTENNAE AND RECEIVERS

A block diagram of the receiving configuration appears in Fig. 1. The antennae used were sections of the east–west arm of the 22.25-MHz T-array of the Dominion Radio Astrophysical Observatory (Costain, Lacey & Roger 1969). Each antenna comprised a sub-array of eight full-wave dipoles with ground screen, 2λ and 2λ, phased to the North Celestial Pole for a polar cap synthesis survey (Dewdney 1978), and with normalized responses of about −17 dB and −7 dB at Cas A upper and lower transit respectively. The centres of the two sub-arrays were separated by 26λ.

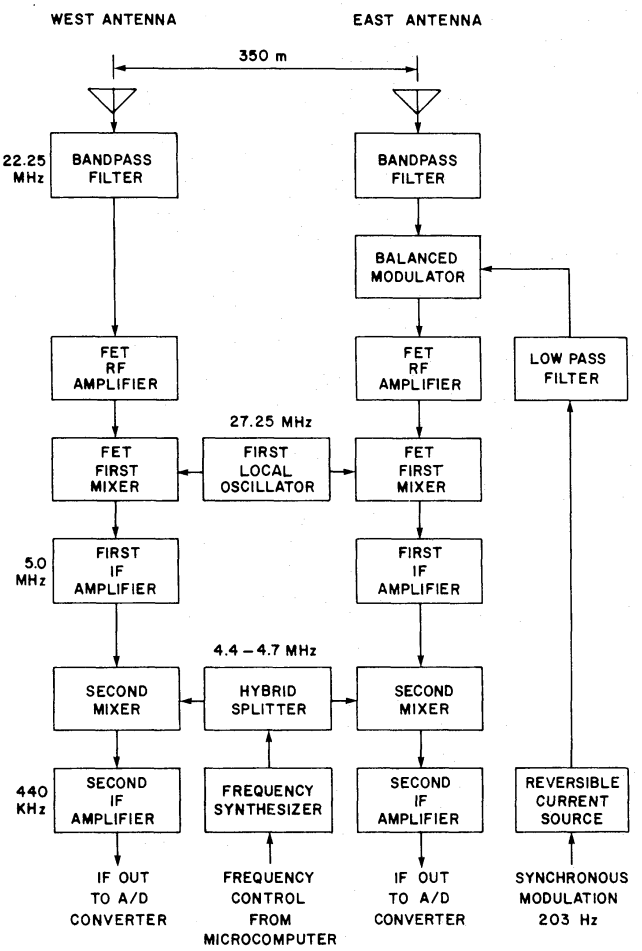

Figure 1. The receiving configuration.

Considerable care was taken to avoid intermodulation distortion. Carefully constructed three-pole input bandpass filters of 5-MHz width gave good rejection far above and far below 22.25 MHz, in particular ~ 100 dB near 1 MHz. FETs were used in the r.f. amplifiers and first mixers to take advantage of their square-law characteristics; the third-order intermodulation intercept point of each channel was −11 dBm. The r.f. amplifiers had 3-dB bandwidths of 600 kHz.

Synchronous modulation of one channel with a bipolar square wave was performed to eliminate the effects of receiver crosstalk. A delay in the modulating waveform was adjusted to make phase transitions coincide with the beginnings of new blocks of FFT samples.

The first local oscillator was distributed from a central point to the front ends of the two channels. Five megahertz i.f. signals were returned from the first i.f. amplifiers to the observatory. Following a second down-conversion, sharply bandlimited signals from 416 to 468 kHz suitable for sampling and A/D conversion were produced.

A frequency synthesizer under control of the microcomputer was used for the second local oscillator. This allowed the spectrum between 22.15 and 22.35 MHz to be divided into four 50-kHz segments, any of which could be selected for observing. The centre frequency could thereby be changed routinely whenever excessive clipping occurred at the A/D converters due to very strong interferers, or whenever too many channels were deleted due to

the presence of a large number of weak interferers. This scheme sufficed to test the merits of frequency changing to reduce interference. No delay compensation to prevent decorrelation was necessary in such a narrow bandwidth.

2.2 THE FFT PROCESSOR

Digital correlation spectrometers which compute power spectra as Fourier transforms of averaged correlation functions have long been used in astronomy. Such correlations are practical when very few bits of quantization are sufficient, since the hardware can be very simple and can operate at high speeds to provide wide bandwidth. At low frequencies, however, wide bandwidth is not essential because radio sources are relatively strong. However, wide dynamic range requiring many bits of quantization is necessary to handle terrestrial interference. This requirement favours spectral analysis by direct Fourier transformation where the computational efficiency of the FFT can reduce the number of expensive arithmetic operations.

A block diagram of the hard-wired FFT processor is shown in Fig. 2. A significant feature affecting the speed of the processor is that, for each FFT performed, both the cross and auto power spectra of the two input waveforms are computed by the action of the output buffer, conjugate multiplier, and adder units. The basis of this feature will now be outlined.

Let $f(n)$ and $g(n)$ be two real series corresponding to the digitized i.f. signals, with $0 \leqslant n \leqslant N-1$. Then, if a complex series $x(n)=f(n)+jg(n)$ is formed, the discrete Fourier transform (DFT) of $x(n)$ will be separable, by the use of the symmetry properties of the DFT, to yield

$$F(m) = \tfrac{1}{2}[X(m) + X^*(N-m)]$$

and

$$G(m) = \frac{-j}{2}[X(m) - X^*(N-m)], \tag{1}$$

where $F(m)$, $G(m)$, and $X(m)$ are the DFTs of $f(n)$, $g(n)$, and $x(n)$, respectively, and $0 \leqslant m \leqslant N-1$ (Stanley 1975). Further, using subscripts r and i to denote the real and imaginary parts of the transform $X(m)$, it follows after algrebraic manipulation that

$$FG^*(m) = \tfrac{1}{2}[X_r(m)\,X_i(N-m) + X_i(m)\,X_r(N-m)] + \frac{j}{4}[X_r^2(m) + X_i^2(m) - X_r^2(N-m) - X_i^2(N-m)] \tag{2}$$

and

$$FF^*(m) = \tfrac{1}{4}[X_r^2(m) + X_i^2(m) + X_r^2(N-m) + X_i^2(N-m) + 2X_r(m)\,X_r(N-m) - 2X_i(m)\,X_i(N-m)], \tag{3}$$

with a relation similar to (3) also available for $GG^*(m)$, but with the signs of the last two terms interchanged. The real part of $FG^*(m)$ is the in-phase cross-spectrum, and the imaginary part is the quadrature cross-spectrum. $FF^*(m)$ and $GG^*(m)$ are the auto-spectra.

The availability of the two auto-spectra allows automatic gain control to be implemented easily. This can be useful when the system noise temperature varies appreciably, with no penalty in the accuracy of the cross-spectra being incurred due to passband ripple when different spectral samples are discarded from moment to moment during the course of interference excising.

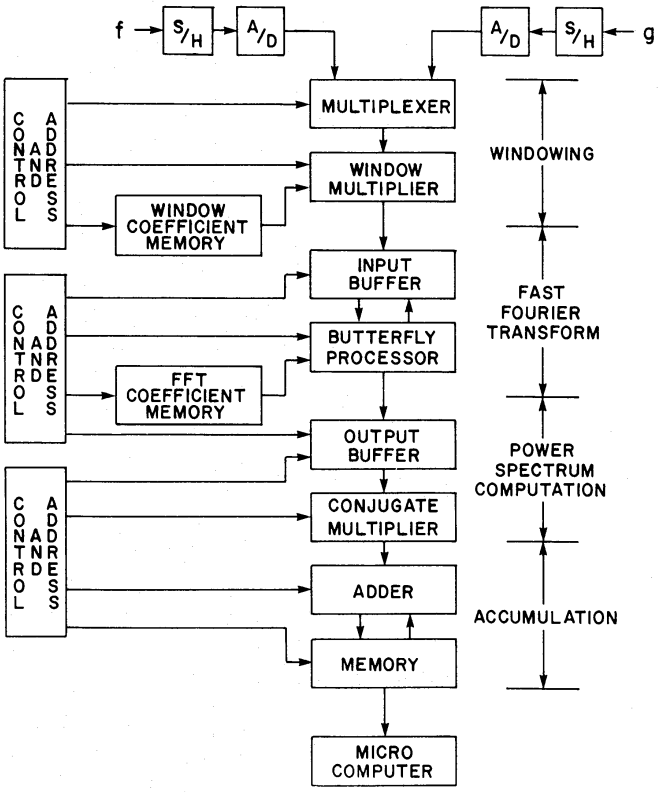

Figure 2. Block diagram of the FFT processor.

The sample-and-hold circuits and 8-bit A/D converters sample the second i.f. outputs at 104 kHz. This process also serves as the third mixing process, converting the signals to baseband.

For real-time operation, the processor has to calculate each 256 point FFT in 2.46 ms. An in-place, decimation-in-time algorithm is performed. The four sections of the output buffer hold $X_r(m)$, $X_i(m)$, $X_r(N-m)$, and $X_i(N-m)$. By gating the correct FFT results from the output buffer in accordance with equations (2) and (3), all four auto- and cross-spectra are computed. After a fixed number of spectra have been accumulated (up to 10^5), the results are transferred to the 6800-microcomputer memory using direct memory access.

Laboratory tests undertaken to verify correct operation of the FFT processor showed that sidelobe levels in the spectra of sinusoidal signals were at least 56 dB below the main lobe. Roundoff noise power in the cross- and auto-spectra increased linearly with input signal power, as expected for block floating-point computation. The anticipated increase in the variance of the means of the cross-spectral due to the Kaiser–Bessel windowing, a factor 2.24, was verified to within 0.5 per cent. The stringent shielding and isolation of the digital sections successfully prevented r.f. leakage into the stages ahead of the A/D converters.

3 Interference excising

In the absence of narrowband interference, the averaged in-phase and quadrature cross-spectral components will exhibit normal probability densities. The means of these spectra will be proportional to the correlated broadband power received from astronomical sources. Narrowband interference may contaminate some of the spectral components. In this case a

robust estimation procedure which is insensitive to statistical outliers must be used to find the means or location parameters θ_C and θ_Q of the underlying normal distributions.

An estimate of the standard deviation σ_X of the underlying distributions is needed for the robust estimation procedure. The ordinary sample standard deviation is relatively inaccurate, even without contamination. A much more accurate estimate of scale can be obtained from the auto-spectra by means of

$$\sigma_X = \sqrt{\frac{\theta_F \theta_G}{2K}}, \tag{4}$$

in which K represents the number of spectra averaged, typically 10^4 to 10^5, and θ_F and θ_G are location parameters for the auto-spectra. These are easily found via the first decile, which is a robust estimator for the centres of the auto-spectra, in as much as it is relatively immune to one-sided contamination.

A simple correction removes the bias of the first decile as used to estimate the mean:

$$\theta_{F,G} = \text{first decile}_{F,G}/(1 - 1.3K^{-1/2}). \tag{5}$$

This estimate is accurate to better than 1 per cent, even with up to 50 per cent contamination by interference. It should be noted that the spectra must be very flat for this estimate to operate properly.

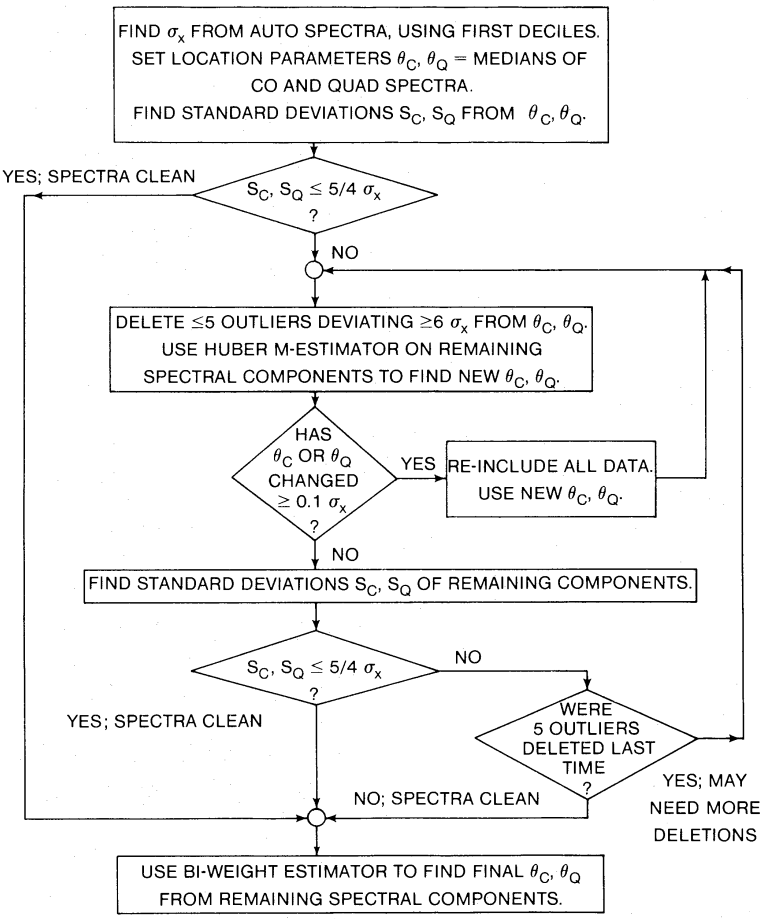

Figure 3. Robust maximum likelihood estimation procedure used to find the location parameters of the cross-spectra.

The estimation method used to find the centres of the cross-spectra, shown in Fig. 3, is a hybrid of three different procedures. The first procedure is a 6σ rejection rule which eliminates large and easily identifiable outliers. The medians of the in-phase and quadrature spectra, being considerably more robust than the means, are taken as initial values for θ_C and θ_Q prior to 6σ rejection. Spectral components directly adjacent to those deviating by more than $6\sigma_x$ are also rejected since they will be contaminated due to leakage during the FFT process. A maximum of five points deviating by more than $6\sigma_x$ is deleted at any one time.

Following deletion, a Huber M-estimator with parameter $k = 1.5$ (Hogg 1979) is used on the remaining points to recalculate θ_C and θ_Q. If it appears that more large outliers are present, additional iterations of 6σ rejections and Huber-estimation are carried out.

The final estimation step is a biweight M-estimator, also described by Hogg. This estimator is one of the best known for finding the centres for contaminated normal distributions. It rejects extreme outliers completely, is insensitive to local groupings of points, and weakens the effect of small changes in individual observations (Hampel 1974). The 6σ rejection and Huber-estimation steps are used to provide reliable initial estimates for the final biweight estimate. Both the Huber and biweight estimators are implemented by means of Newton–Raphson iteration.

An earlier version of the FFT processor used fixed-point arithmetic and calculated only the in-phase portion of the cross-power spectrum (Kasper *et al.* 1978). The interference-excising method used was simple iterative 3σ rejection. This method is satisfactory for large interferers, but not for low-level contamination, which prompted the development of the more sophisticated robust estimation technique described above. During field tests of the present system, on-line deletions of interference used a simple 4σ rejection rule and the resultant fringes were displayed on a chart recorder. The raw averaged spectra were also recorded on magnetic tape, allowing subsequent off-line analysis. With appropriate programming, the robust estimation algorithm of Fig. 3 could easily have been carried out by the on-line microcomputer.

At this point, the possible effects of scintillation on an interference-excising system such as the one described here should be mentioned. Spectral features of width ~ 1 kHz can occur, especially at longer decametric wavelengths because of the fourth-power dependence of decorrelation bandwidth on observing frequency (Sutton 1971). But the effect of deleting spurious spectral features from the cumulative spectra would not be large; $3N/4$ samples would have to be excised before σ_x would double. Furthermore, the intensity of any given spectral feature would appear reduced by the factor by which the accumulation time exceeded the decorrelation time of scintillation features. On the other hand, spectral features of width considerably greater than the interval between spectral samples could produce individual spectra which are rougher, making detection of interferers ultimately more difficult, and possibly vitiating (5). The importance of scintillation during a particular observation would depend on the relative magnitudes of the product of antenna temperature and scintillation index of the source, and the system temperature itself.

4 Observations

Data were collected during the period 1979 November 12 to 1980 January 6. An example of raw fringes taken at sunrise, November 29, appears in Fig. 4. The peaks are actually truncated to ±100, whereas some were in reality as large as ±1000. Since the interfering signal was often contained predominantly in a single spectral channel (e.g. a c.w. telephony signal of 100-Hz bandwidth) and it is the means of the spectra which are displayed, then

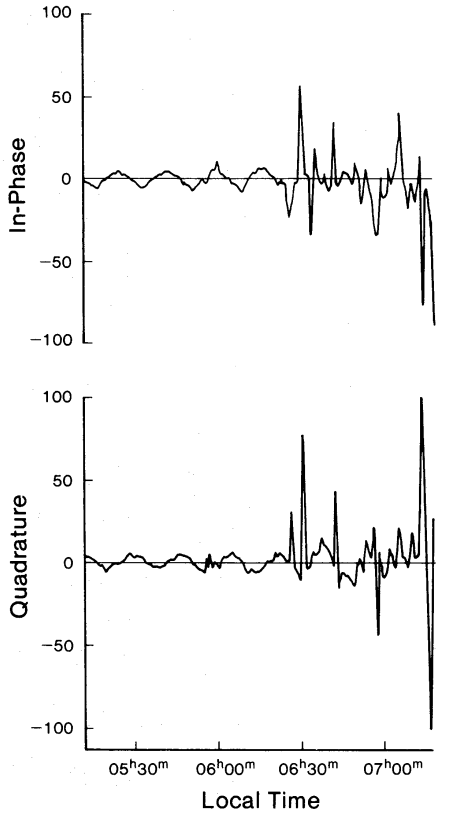

Figure 4. Fringes from Cas A recorded at sunrise, 1980 November 29, without interference excision.

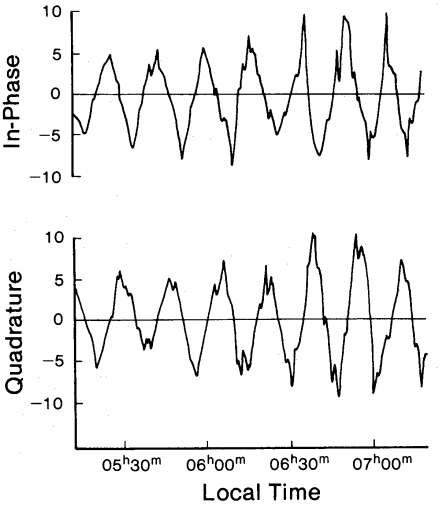

Figure 5. Fringes of Fig. 4, after interference excision. Note change of scale.

occasionally the interferer must have been $\gtrsim 40$ dB larger than the fringes, which are $\lesssim 10$ in amplitude on this arbitrary scale.

Fig. 5 shows the same fringes after application of the robust M-estimator algorithm, and they are shown again in Fig. 6 in polar form after smoothing in blocks of 60 min and removal of slow gain variations. There is a change in scale between Figs 4 and 5.

The frequency-changing capability of the microcomputer-controlled second local oscillator was used to choose among four adjacent 50-kHz channels between 22.15 and

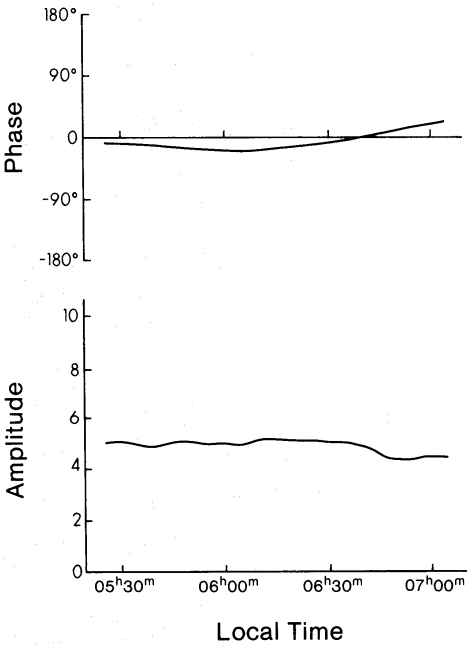

Figure 6. Fringes of Fig. 5 in polar form after smoothing and removal of slow gain variations.

22.35 MHz. The frequency was changed whenever excessive clipping occurred or when more than 40 per cent of spectral components were deleted. The frequency-changing capability was judged to be of limited value, at least during daytime observations near solar maximum. Interference levels were occasionally high enough to cause serious intermodulation, noticeable on a spectrum analyser monitoring the first i.f. outputs, and in addition, broad-band (sometimes > 100-kHz wide) sweeping interferers were sometimes encountered. The system spent essentially all of the time in the two lower 50-kHz channels, since these consistently exhibited far less interference than the upper ones. Automatic frequency-changing could be of greatest benefit if channels had roughly equal and independent probabilities of containing interference. Such was not the case at the frequencies used in this trial.

A significant problem noted during daytime was the presence of sweeping interference, believed to originate from ionospheric sounding transmitters. The present system relies upon the frequencies of the interferers remaining fixed.

A great deal of interference was received and deleted during the nights, as well as during mornings and evenings. The incidence of night-time interference varied during the observing period, however. Often, low-level interference, which would not be noticeable in records taken with a conventional receiving system, was revealed by the deletion of appreciable numbers of spectral samples. Between November 20 and 30, low-level interference was virtually continuous each night, but the nights of December 5 and 6 were free of interference. The remainder of the records showed intervals of low-level night-time interference lasting from a few minutes to many hours. Interference-removal consistently allowed from 60 to 90 min additional observing time (occasionally more) in the mornings and in the evenings.

5 Conclusions

This work has demonstrated that interference-excising is successful during the winter of a solar maximum. From an interference standpoint, daytime in the winter of a solar maximum

is the worst possible time to attempt low-frequency radio astronomy. Overall, the interference-excising system performed very well as long as interference levels were not so high as to cause intermodulation. Generally this was the case for periods of from 60 to 90 min in both the mornings and evenings when interference was increasing or decreasing, and interference was also removed on the numerous occasions when low-level interference was encountered during the night.

The excising system operated at times with up to 50 per cent of spectral components being deleted because of interference. More typically, successful operation was possible with 20–30 per cent of the overall bandwidth being rejected.

The main question which arises is how well such a system could operate during solar minimum when conditions are more favourable for low-frequency radio astronomy. Since typical critical frequencies, even during summer days of a solar minimum, are no higher than those during winter nights of a solar maximum, it is likely that interference excising could allow for very long periods of continuous interference-free observing during both summer and winter of a solar minimum.

Acknowledgments

We thank the staff of the Dominion Radio Astrophysical Observatory for their generosity in making the 22.25-MHz array available for this experiment, and in particular Drs P. E. Dewdney and R. S. Roger for their encouragement and help during field testing. We also thank Dr J. F. Vaneldik and Mr P. Haswell of the University of Alberta for their advice and assistance. This work was supported by research grants from the Natural Sciences and Engineering Research Council of Canada. One of us (B.L.K.) acknowledges receipt of an NSERC studentship.

References

Braude, S. Ya., Lebedeva, O. M., Megn, A. V., Ryabov, B. P. & Zhouk, I. N., 1969. *Mon. Not. R. astr. Soc.*, **143**, 289.
Costain, C. H., Lacey, J. D. & Roger, R. S., 1969. *Publ. Dominion Obs.*, **25**, 327.
CCIR Report AM/2, Study Group 6, 1976. *Ionospheric limitations to ground-based astronomy.*
Dewdney, P. E., 1978. *PhD thesis,* University of British Columbia.
Duffett-Smith, P. J., 1980. *Mon. Not. R. astr. Soc.*, **190**, 139.
Ellis, G. R. A. & Hamilton, P. A., 1966. *Astrophys. J.*, **143**, 227.
Ershov, A. A., 1979. *Automn remote Control,* **39**, 1152.
Hamilton, P. A. & Haynes, R. F., 1968. *Aust. J. Phys.*, **21**, 895.
Hampel, F. R., 1974. *J. Am. statist. Ass.*, **69**, 383.
Hogg, R. V., 1979. *Am. Statistn,* **33**, 108.
Huber, P. J., 1964. *Ann. math. Statist.*, **35**, 73.
Kasper, B. L., 1981. *PhD thesis,* University of Alberta.
Kasper, B. L., Chute, F. S., Routledge, D. & Vaneldik, J. F., 1978. *J. R. astr. Soc. Can.*, **72**, 310.
Shain, C. A. 1958. *Proc. IRE,* **46**, 85.
Stanley, W. D., 1975. *Digital Signal Processing,* Reston Publishing Co., Reston, Virginia.
Sutton, J. M., 1971. *Mon. Not. R. astr. Soc.*, **155**, 51.
Wheeler, J. L., 1977. *IEEE Trans. Electromagnetic Compatibility,* **EMC-19**, 132.